JCTC Journal of Chemical Theory and Computation

Accurate Spin-State Energies for Iron Complexes

Marcel Swart*

Institució Catalana de Recerca i Estudis Avançats (ICREA), Pg. Lluís Companys 23, 08010 Barcelona, Spain, and Institut de Química Computacional and Departament de Química, Universitat de Girona, Campus Montilivi, 17071 Girona, Spain

Abstract: A critical assessment of the OPBE functional is made for its performance for the geometries and spin-states of iron complexes. In particular, we have examined its performance for the geometry of first-row transition-metal (di)halides (MnX_2, FeX_2, CoX_2, NiX_2, CuX, X=[F, Cl]), whose results were previously [*J. Chem. Theory Comput.* **2006**, *2*, 1282] found to be representative for a much larger and more diverse set of 32 metal complexes. For investigating the performance for spin ground-states of iron complexes, we examined a number of small iron complexes ($Fe(II)Cl_4^{2-}$, $Fe(III)Cl_4^{1-}$, $Fe(II)Cl_6^{4-}$, $Fe(III)Cl_6^{3-}$, $Fe(II)CN_6^{4-}$, $Fe(III)CN_6^{3-}$, $Fe(VI)O_4^{2-}$, $Fe(III)(NH_3)_6^{3+}$), benchmark systems ($Fe(II)(H_2O)_6^{2+}$, $Fe(II)(NH_3)_6^{2+}$, $Fe(II)(bpy)_3^{2+}$), and several challenging iron complexes such as the $Fe(II)(phen)_2(NCS)_2$ spin-crossover compound, the monopyridylmethylamine $Fe(II)(amp)_2Cl_2$ and dipyridylmethylamine $Fe(II)(dpa)_2^{2+}$, and the bis complex of Fe(III)-1,4,7-triazacyclononane ($Fe(III)(^9aneN_3)_2^{3+}$). In all these cases OPBE gives excellent results.

Introduction

The reliable prediction of the spin ground-state of transition-metal complexes remains a challenging task,[1] both for theory and experiment. On the experimental side, the situation may be complicated by ligand-exchange reactions,[2] dimerization processes, oxidation/reduction, impurities, etc. Moreover, the structural characterization of the complexes may be hampered by problematic crystallization, reduced lifetimes of transient species (such as the elusive complex I in the catalytic cycle of cytochrome P450),[3−6] or temperature-dependences of the population of the different spin-states. The latter is for instance observed in spin-crossover compounds[7] whose structures may not be resolved at all temperatures. In principle, theory should be able to help with the interpretation of the experimental data, predict the spin ground-state, and help to determine reaction mechanisms. However, theory is not without its own problems. The most accurate *ab initio* theoretical methods (CCSD(T), MR-CI) are too demanding for everyday use and in some cases (such as CASPT2) need expert knowledge of the methodology. More efficient are calculations based on density functional theory (DFT),[8] but the results are shown to depend largely on the choice of DFT functional that is being used.

This is in particular true for the calculation of spin-state splittings,[1] where standard pure functionals (like LDA,[9] BLYP,[10,11] or PBE[12]) systematically overstabilize low-spin states, while hybrid functionals (e.g., B3LYP,[13,14] PBE0[15]) overstabilize high-spin states due to the inclusion of a portion of Hartree−Fock exchange. The problems with B3LYP in correctly describing the relative energies of the spin states of iron complexes led Reiher and co-workers to propose a new functional (dubbed B3LYP*),[16] in which the amount of HF exchange was lowered to 15% (instead of 20% in B3LYP). For many systems, this reduction indeed improves the B3LYP results,[17] apparently without sacrificing the good performance for organic systems.[17] However, it was not successful for all iron complexes,[18,19] as for instance is the case for the $Fe(phen)_2(NCS)_2$ spin-crossover compound. A further reduction to 12% of HF exchange seems necessary[18] to give good results for this particular iron complex. Therefore, with B3LYP and B3LYP*, it is *a priori* unknown if the amount of HF exchange is appropriate for the transition-metal complex under study, which is an undesirable situation.

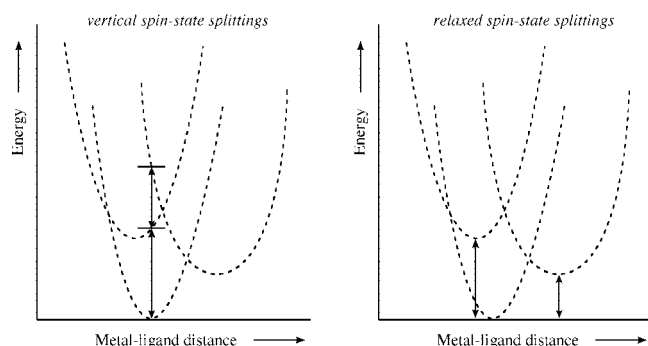* Corresponding author fax: +34-972-183241; e-mail: marcel.swart@icrea.es.

Figure 1. Schematic representation of *vertical* (left-side) and *relaxed* (right-side) spin-state splittings.

Recently, we made a systematical investigation of the influence of the functional[1] and of the basis set[20] on the relative spin-state energies (i.e., the spin-state splittings[21]) for a number of iron complexes. The influence of the basis set was found to be substantial. In principle, with an infinitely large basis set, both Slater-type orbital (STO) and Gaussian-type orbital (GTO) series should converge to the same final answer, which is indeed what we observed for both vertical and relaxed spin-state splittings (see Figure 1 for the difference between vertical and relaxed spin-state splittings). However, we found that the STO basis sets give consistent and rapidly converging results, while the convergence with respect to the basis set size is much slower for the GTO basis sets. Very demanding basis sets like Dunning's correlation consistent (cc-pVTZ, cc-pVQZ) were needed to achieve good results, especially for relaxed spin-state split-tings.[20] Furthermore, the use of basis sets containing effective core potentials (ECPBs) resulted in spin-state splittings that are systematically different from the STO-GTO results.

From these and related studies,[1,22,23] it became clear that recent and improved functionals provide more accurate results. This is in particular true for the functionals containing Handy and Cohen's optimized exchange (OPTX) func-tional,[24] such as OLYP or OPBE.[25] The latter OPBE functional provided the correct spin ground-state for vertical spin-state splittings of a number of Fe(II) and Fe(III) complexes,[1] which is corroborated by good results obtained more recently in studies from other groups.[6,19,22,23,26−35] This good performance of OPBE (and the related OLYP) concurs with recent benchmark studies on the energy profiles of nucleophilic substitution reactions[36] and on the NMR chemi-cal shifts of organic molecules.[27,28] In the former, it was shown that the underestimation of reaction barriers by standard pure DFT functionals is dramatically reduced by using OPBE, while for the NMR chemical shifts its performance is significantly better than other DFT functionals (including B3LYP) and surpasses many times even the *ab initio* MP2 method.

Han and Noodleman recently used a series of small iron complexes to obtain the Mössbauer isomer shift parameters for OPBE and OLYP,[37] which were subsequently used to study the intermediate Q of the hydroxylase component of soluble methane monooxygenase (MMOH).[38] They showed that OPBE (and OLYP) do not overestimate the Fe-ligand covalency for these model structures, in contrast to the PW91 functional. Moreover, OPBE and OLYP correctly predicted

the high-spin antiferromagnetically (AF) coupled Fe^{4+} sites. Furthermore, in a series of papers Ghosh and co-workers[23,39−45] have clearly demonstrated that OPBE (and OLYP) seems to be giving good results not only for iron complexes but also for other transition metals.

In the present contribution, we make an assessment of the OPBE functional for the spin-states of iron complexes. Apart from studying its accuracy for the geometries of transition-metal complexes, we investigate the spin ground-states of small iron complexes like $Fe(CN)_6^{3-}$, and challenging iron complexes such as the $Fe(phen)_2(NCS)_2$ spin-crossover compound, and compare the results of OPBE with other functionals. Moreover, a comparison is made with benchmark *ab initio* data obtained with high-level CASPT2 methods, where available. Finally, using an energy decomposition analysis the origin of the spin ground-state of these com-plexes is explained in terms of a compromise between metal−ligand bonding and Hund's rule of maximum multiplicity.

Computational Details

Most DFT calculations were performed with the Amsterdam Density Functional (ADF) suite of program.[46,47] MOs were expanded in an uncontracted set of Slater type orbitals (STOs)[48] of triple-ζ quality containing diffuse functions and one (TZP) or two (TZ2P) sets of polarization functions. Core electrons (1s for second period, 1s2s2p for third-fourth period) were not treated explicitly during the geometry optimizations (frozen core approximation[46]), as it was shown[49] to have a negligible effect on the obtained geom-etries. An auxiliary set of s, p, d, f, and g STOs was used to fit the molecular density and to represent the Coulomb and exchange potentials accurately for each SCF cycle.

Energies and gradients were calculated using the local density approximation (LDA; Slater exchange and VWN correlation[9]) with gradient-corrections (GGA) for exchange (OPTX[24]) and correlation (PBE[50,51]) included self-consis-tently, i.e. the OPBE functional. Geometries were optimized with a locally adapted version of the QUILD program[52,53] using adapted delocalized coordinates[52] until the maximum gradient component was less than $1.0 \cdot 10^{-4}$ a.u. Single point energies for all other DFT functionals were obtained (post-SCF within the METAGGA scheme) at the OPBE optimized geometries using the corresponding all-electron basis sets.

As the gradients for hybrid functionals are not yet available within the ADF program, the geometries of the first-row transition-metal (di)halides were also obtained with the NWChem program (version 5.0)[54] for a number of DFT functionals (OPBE, B3LYP, BP86, PBE, B3LYP*) using the cc-pVTZ[55] basis set of Gaussian-type orbitals (GTOs).

For some of the iron complexes in this paper, we included solvent effects through the use of a dielectric continuum (COSMO[56,57]) model, with the appropriate dielectric con-stants (ϵ) and solvent radii (R_{solv})[58] for the solvent used. A nonempirical approach[59] to including solvent effects in QM calculations has been used, which works well for solvation processes.[58,59]

Energy Decomposition Analysis. The total energy ΔE_{total} for the heterolytic association[19] reaction between the iron(II)

Accurate Spin-State Energies

J. Chem. Theory Comput., Vol. 4, No. 12, 2008 **2059**

cation and n ligands L with charge q (Fe^{2+} + n·L^q → FeL$_n^{nq+2}$) results directly from the Kohn−Sham molecular orbital (KS-MO) model[60] and is made up of two major components (eq 1):

$$\Delta E_{\text{total}} = \Delta E_{\text{prep}} + \Delta E_{\text{int}} \qquad (1)$$

In this formula, the preparation energy ΔE_{prep} is the energy needed to prepare the (ionic/neutral) fragments and consists of three terms (eq 2):

$$\Delta E_{\text{prep}} = \Delta E_{\text{deform}} + \Delta E_{\text{lig−lig}} + \Delta E_{\text{valexc}} \qquad (2)$$

The first is the energy needed to deform the separate molecular fragments (in this case only for the ligands) from their equilibrium structure to the geometry that they attain in the overall molecular system (ΔE_{deform}). The second ($\Delta E_{\text{lig-lig}}$) is the interaction energy between the ligands when they are placed at the geometry of the molecule (but without the iron present) to make one fragment file that contains all ligands. This interaction results mainly from electrostatic repulsion in case of negatively charged ligands. The third term (ΔE_{valexc}) is the valence-excitation energy needed to prepare the metal from its atomic spin-unrestricted (polarized) ionic ground-state to the spin-restricted (polarized) ionized form. The valence-excitation energy consists of two terms: the first (positive, e.g. destabilizing) term is the energy difference between the spin-polarized metal cation in its ground state (e.g., the quintet ^{5}D state for Fe^{2+}) and the spin-restricted, nonpolarized (singlet) cationic form used for the metal cation fragment (the fragments need to be spin-restricted). For the ground-state of the cation, we use the "average of configuration" approach,[61] which gives an approximate single-determinant description of the true atomic spin ground-state. Note also that the metal cation fragment is prepared with the occupation of the orbitals it attains in the molecule, i.e. it does not necessarily, and usually does not, correspond to the isolated metal cation. As a result, the ΔE_{valexc} values cannot be compared directly with experimental excitation energies for the metal cation (see also refs 61 and 62). The second term results from preparing (polarizing) the cation fragment with the multiplet state it attains in the metal complex; this term is negative (stabilizing) for triplet and quintet and zero for singlet states. It is achieved by changing the occupations of the fragment orbitals. For instance for iron(II), the spin-restricted cationic fragment would be prepared with 3 α and 3 β d-electrons; within the molecule calculation, the occupations of the iron-fragment are changed to make 4 α and 2 β d-electrons for a triplet state or to 5 α and 1 β d-electrons for a quintet state. There is a discrepancy (of ca. 2 kcal mol^{-1}) between the interaction energy thus obtained from these fragments (*vide infra*) and the change in energy when going from the isolated ligands and (spin-unrestricted, polarized) metal cation to the metal complex. This difference results from the fact the α and β orbitals are kept the same in the former (fragment) approach, while they are allowed to relax in the latter. There are two possibilities to deal with this discrepancy, either to make this energy difference part of the preparation energy (as done here) or to scale the interaction energy components accordingly (values reported in the Supporting Information, Tables

S1 and S2). However, this energy difference is generally negligible compared to the interaction energy components and is therefore of no consequence for the importance of the components of the interaction energy. For the interested reader, the EDA analysis for the Fe(amp)$_2$Cl$_2$ complex has been performed also with the BP86 functional (see the Supporting Information). Although it induces a slight change in the values for the different energy components, this does not influence the importance of the compromise between Hund's rule of maximum multiplicity and metal−ligand covalent interactions for the determination of the spin ground-state of these molecules (*vide infra*).

The interaction energy ΔE_{int} is the energy released when the prepared fragments (i.e., Fe^{2+} + n·L^q) are brought together into the position they have in the overall molecule. It is analyzed for our model systems in the framework of the KS-MO model[60] using a Morokuma-type[63] decomposition into electrostatic interaction, Pauli repulsion (or exchange repulsion), and (attractive) orbital interactions (eq 3).

$$\Delta E_{\text{int}} = \Delta V_{\text{elstat}} + \Delta E_{\text{Pauli}} + \Delta E_{\text{orbint}} \qquad (3)$$

The term ΔV_{elstat} corresponds to the classical electrostatic interaction between the unperturbed charge distributions of the prepared (i.e., deformed) fragments and is usually attractive. The Pauli-repulsion, ΔE_{Pauli}, comprises the destabilizing interactions between occupied orbitals and is responsible for the steric repulsion. The orbital interaction ΔE_{orbint} in any MO model, and therefore also in Kohn−Sham theory, accounts for electron-pair bonding, charge transfer (i.e., donor−acceptor interactions between occupied orbitals on one fragment with unoccupied orbitals of the other, including the HOMO−LUMO interactions), and polarization (empty-occupied orbital mixing on one fragment due to the presence of another fragment). In the case of metal complexes with symmetry, the orbital interaction energy can be further decomposed into the contributions from each irreducible representation Γ of the interacting system (eq 4) using the extended transition state (ETS) scheme developed by Ziegler and Rauk.[64,65]

$$\Delta E_{\text{orbint}} = \sum_{\Gamma} \Delta E_{\Gamma} \qquad (4)$$

Results

Here we report a critical assessment of the OPBE functional for its performance for the geometries and spin-states of iron complexes. Spin contamination is in all cases negligible, as shown by the expectation values for S^2 that are very close to the pure spin-state values. No attempt at spin-projection[66,67] has therefore been made, as these corrections would not alter the energies significantly.

Geometry Optimization of (Di)halides. We have examined the performance of OPBE for the structure of first-row transition-metal (di)halides (MnX$_2$, FeX$_2$, CoX$_2$, NiX$_2$, CuX, X=[F, Cl]), whose results were found[68] to be representative for a much larger and more diverse set of 32 metal complexes. For the geometry optimization of these (di)ha-

***Table 1.*** Metal-Halide Distances (Å) and Mean Absolute Deviations (MAD, Å) for a Set of 10 (Di)halides

compd (mult[a])	exp.	OPBE TZ2P[b]	OPBE cc-pVTZ[c]	BP86 TZ2P[b]	BP86 cc-pVTZ[c]	PBE TZ2P[b]	PBE cc-pVTZ[c]	B3LYP cc-pVTZ[c]	B3LYP* cc-pVTZ[c]
MnF_2 (6)	1.797	1.793	1.788	1.790	1.790	1.794	1.789	1.796	1.793
FeF_2 (5)	1.755	1.757	1.750	1.752	1.752	1.755	1.751	1.757	1.755
CoF_2 (4)	1.738	1.720	1.713	1.725	1.716	1.728	1.715	1.720	1.717
NiF_2 (3)	1.715	1.719	1.710	1.711	1.710	1.714	1.709	1.730	1.728
CuF (1)	1.745	1.759	1.758	1.747	1.753	1.752	1.751	1.761	1.757
$MnCl_2$ (6)	2.184	2.162	2.166	2.169	2.173	2.168	2.171	2.194	2.188
$FeCl_2$ (5)	2.128	2.117	2.121	2.123	2.127	2.123	2.125	2.132	2.126
$CoCl_2$ (4)	2.090	2.072	2.076	2.077	2.082	2.077	2.080	2.104	2.098
$NiCl_2$ (3)	2.056	2.045	2.047	2.050	2.054	2.051	2.053	2.073	2.067
$CuCl$ (1)	2.052	2.044	2.061	2.050	2.066	2.051	2.064	2.089	2.083
MAD		0.011	0.011	0.007	0.008	0.006	0.009	0.014	0.011

[a] Experimentally (and theoretically) observed multiplicity for this complex. [b] STO basis set. [c] GTO basis set.

lides, we used both a STO (TZ2P) and a GTO (cc-pVTZ) basis set to be able to compare directly with literature data that have been obtained with GTO basis sets. The dihalide molecules were treated as linear molecules ($D_{\infty h}$ symmetry), as observed experimentally. The obtained distances with both basis sets and a number of functionals are reported in Table 1. In the original paper by Bühl and Kabrede,[68] the best results were obtained by pure GGA (BPW91, BP86) and metaGGA (TPSS) functionals, with mean absolute deviations (MAD) from experimental data of 0.008−0.009 Å when using the AE1 basis. This GTO basis set consists of the augmented all-electron Wachters basis set on the metal and 6−31G* on the halides. For BP86 and B3LYP, the MAD values obtained here with the cc-pVTZ basis set are similar to the ones obtained with this AE1 basis, with values for BP86 of 0.008 Å (cc-pVTZ) and 0.009 Å (AE1), while for B3LYP they are 0.014 Å (cc-pVTZ) and 0.015 Å (AE1).

The OPBE functional is shown to be less accurate than BP86 but more accurate than B3LYP, with MAD values of 0.011 Å for both the TZ2P and the cc-pVTZ basis set (see Table 1). The same value is observed for the B3LYP* functional with the cc-pVTZ basis (see Table 1). Also the maximum error is significantly smaller for OPBE (0.025 Å with the cc-pVTZ basis, 0.022 Å with TZ2P) compared to B3LYP* (0.032 Å cc-pVTZ) and B3LYP (0.038 Å cc-pVTZ) and again only slightly larger than the most accurate functionals BP86 (0.022 Å with both cc-pVTZ and AE1) and TPSS (0.022 Å, AE1 basis). Therefore, the OPBE functional seems to provide a good description for the geometries of transition-metal complexes, with an accuracy that is close to that of the best functionals and significantly better than other functionals, such as BLYP, B3LYP, or VS98.[68]

Benchmark Systems for Spin-State Splittings. Recently, Pierloot and co-workers reported a benchmark study[69,70] on a set of three iron complexes ($Fe(H_2O)_6^{2+}$, $Fe(NH_3)_6^{2+}$, $Fe(bpy)_3^{2+}$, see Scheme 1), which were investigated with high-level CASPT2 calculations and, for comparison, with Hartree−Fock (HF) and a number of DFT functionals (LDA, BP86, B3LYP, PBE0), following up on earlier studies on these complexes.[62,71−73] Because of the absence of electron correlation for electrons with unlike spins in HF, this method unduly favors high-spin states too much,[19] which shows up clearly in their results. For all three complexes HF predicts a high-spin state, mistakenly also for the low-spin bipyridyl

Scheme 1. Benchmark Iron Complexes $Fe(H_2O)_6^{2+}$, $Fe(NH_3)_6^{2+}$, and $Fe(bpy)_3^{2+a}$

$Fe(H_2O)_6^{2+}$ $Fe(NH_3)_6^{2+}$ $Fe(bpy)_3^{2+}$
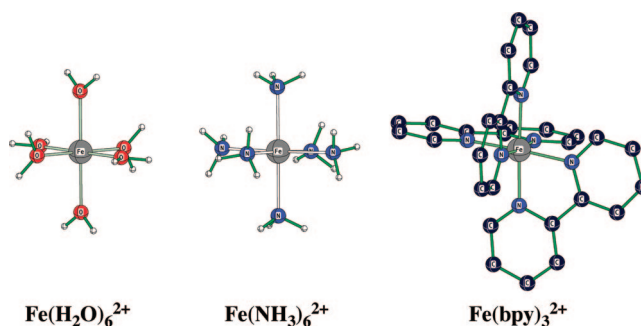
[a] Hydrogens were omitted for clarity.

complex, and with a large deviation from the reference CASPT2 ΔE_{HL} values (see Table 2). The overstabilization of low-spin states by standard pure functionals[1] is reconfirmed by their data for LDA and BP86[69] and for RPBE in another study by Deeth and Fey.[71] Interestingly, the BP86 functional still predicts the correct spin ground-state for all three molecules, i.e. a high-spin state for $Fe(H_2O)_6^{2+}$ and $Fe(NH_3)_6^{2+}$ and a low-spin state for $Fe(bpy)_3^{2+}$, albeit with a large deviation (ca. 15 kcal mol^{-1}) from the reference CASPT2 data. Although this deviation is smaller for the hybrid B3LYP and PBE0 functionals with a value of respectively 11 and 9 kcal mol^{-1}, these latter two functionals fail to predict the correct spin ground-state for the bipyridyl complex.[69]

These systems have been investigated with the OPBE functional using the TZP and TZ2P (STO) basis sets (see Table 2). The calculations were performed within D_3 symmetry for the ammonia and bipyridine complexes and within C_i with water as ligand, in order for a fair comparison with the best available CASPT2 data that were obtained with the same symmetry constraints. For the quintet (and triplet) state of the water complex this leads to Jahn−Teller distortions, similar to the CASPT2 study by Pierloot and co-workers. The symmetry constraints for the triplet states, for which no CASPT2 data are available to compare with, are for all three complexes the same as those of the singlet and quintet states. One of the reviewers pointed out that these triplet and quintet states are formally Jahn−Teller active, and lower energies might be obtained by allowing Jahn−Teller

Accurate Spin-State Energies

J. Chem. Theory Comput., Vol. 4, No. 12, 2008 **2061**

Table 2. Spin-State Splittings ΔE (kcal mol^{-1})^a for Benchmark Iron Complexes

	Fe(H$_2$O)$_6^{2+}$			Fe(NH$_3$)$_6^{2+}$			Fe(bpy)$_3^{2+}$			
	sing	trip	quin	sing	trip	quin	sing	trip	quin	*MAD^b*
CASPT2^{c,d}	46.6	n/a^e	0	20.3	n/a^e	0	0	n/a^e	13.2	-
HF^c	81.1	n/a^e	0	72.8	n/a^e	0	0	n/a^e	−70.5	*56.9*
LDA^c	9.6	n/a^e	0	−22.4	n/a^e	0	0	n/a^e	61.9	*42.8*
BP86^c	28.4	n/a^e	0	5.1	n/a^e	0	0	n/a^e	23.2	*14.5*
RPBE ^{f}	34.3	n/a^e	0	6.3	n/a^e	0	0	n/a^e	29.9	*14.3*
B3LYP^c	33.1	n/a^e	0	14.1	n/a^e	0	0	n/a^e	−0.6	*11.2*
PBE0^c	46.0	n/a^e	0	24.7	n/a^e	0	0	n/a^e	−9.0	*9.1*
OPBE^g	48.6	36.8	0	19.5	35.2	0	0	25.9	13.3	*1.0*
OPBE^h	49.3	37.0	0	19.0	35.1	0	0	26.5	14.9	*1.9*

^{a} Relative to experimental spin ground-state, using D_3 symmetry for the ammonia and bipyridine complexes, and C_i symmetry with water as ligand. ^{b} Mean absolute deviation (MAD) of ΔE_{HL} with respect to reference CASPT2 data. ^{c} From ref 69. ^{d} CAS[10,12] space with atomic natural orbitals (ANO) basis sets, contracted to [7s6p5d3f2g1h] on Fe, [4s3p2d1f] on N and O, and [3s1p] on H. ^{e} Not available, triplet state was not considered in refs 69 and 71. ^{f} From ref 71. ^{g} This work, obtained with TZP (STO) basis set. ^{h} This work, obtained with TZ2P (STO) basis set.

Table 3. Spin-State Energies (ΔE, kcal mol^{-1})^a and Iron-Ligand Distances (R, Å) for Small Iron Complexes

	low spin		interm spin		high spin	
compd	ΔE	R	ΔE	R	ΔE	R
Fe(II)F$_4^{2-b}$	81.9	1.980	42.3	2.015	0	2.021
Fe(II)Cl$_4^{2-b}$	80.6	2.310	39.3	2.363	0	2.381
Fe(II)Cl$_4^{2-c}$	*80.4*	*2.237, 2.321*	*36.1*	*2.331, 2.361*	*0*	*2.383, 2.383*
Fe(II)Br$_4^{2-b}$	71.0	2.446	37.8	2.526	0	2.545
Fe(II)(CN)$_6^{4-d}$	0	1.919	51.8	2.126	38.7	2.419
Fe(III)F$_4^{1-b}$	75.4	1.798	53.4	1.828	0	1.842
Fe(III)Cl$_4^{1-b}$	60.1	2.144	40.8	2.195	0	2.218
Fe(III)Br$_4^{1-b}$	57.4	2.306	37.3	2.370	0	2.386
Fe(III)(CN)$_6^{3-d}$	0	1.925	48.2	2.092	45.9	2.234
Fe(III)(NH$_3$)$_6^{+3e}$	7.4	2.055	18.8	2.173	0	2.239
Fe(VI)O$_4^{2-b}$	17.2	1.663	0	1.663	50.1	1.728

^{a} Relative to experimental spin ground-state. ^{b} Using T_d symmetry. ^{c} Using C_{2v} symmetry. ^{d} Using O_h symmetry. ^{e} Using D_3 symmetry.

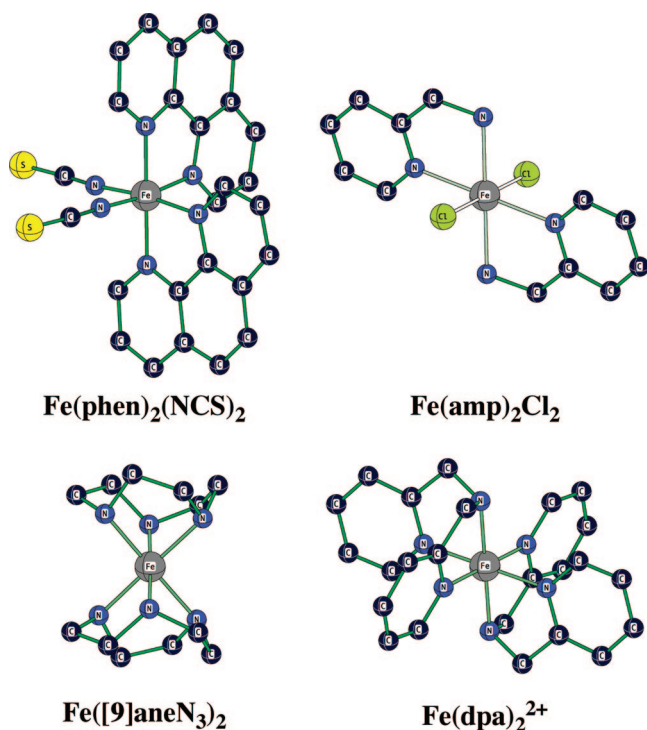distortions to take place. For the bipyridine complex, this indeed does seem to be the case, but the energy gain is only about 100−200 cm^{-1} (ca. 0.3−0.6 kcal·mol^{-1}) for the quintet state of the bipyridyl complex.[69] For the ammonia complex, the Jahn−Teller distortions seem to lead to similarly small energy differences; however, in this case the energy of the quintet state goes up in energy at the CASPT2[10,12]//PBE0 level.[69] In any case, here the comparison is made with the best available reference CASPT2 energies, for which Jahn−Teller distortions were not taken into account. The conformations of the ammonia and water ligands in these calculations correspond to those used in the CASPT2 study by Pierloot and co-workers, which therefore enables a fair comparison between the OPBE and CASPT2 results. Furthermore, the vibrational frequencies of these complexes were calculated, which resulted in all-positive frequencies. For all three complexes OPBE predicts the correct spin ground state, i.e. a quintet for Fe(H$_2$O)$_6^{2+}$ and Fe(NH$_3$)$_6^{2+}$ and a singlet for Fe(bpy)$_3^{2+}$. Moreover, the deviation from the reference CASPT2 data is rather small with values of 1.0 kcal mol^{-1} (TZP basis) and 1.9 kcal mol^{-1} (TZ2P basis), i.e. a significant reduction by an order of magnitude compared to the values from the other functionals. The OPBE deviations with both basis sets fall well within the estimated accuracy of the CASPT2 data (~1000 cm^{-1} or 2.9 kcal mol^{-1}) and therefore clearly show the excellent performance of the OPBE functional.

Spin States of Small Iron Complexes. Next, we investigated a set of small molecules that had been studied previously (partly) by Noodleman,[37] Deeth,[71] Neese,[74] and Filatov[75] (among others) for the description of Mössbauer spectroscopy of these complexes. The predicted spin-state splittings for some of the small complexes by OPBE are reported in Table 3, which confirms the correctness[37] of the OPBE functional for providing spin ground states of iron complexes. Surprisingly, the correct description of the spin ground-state of most of these molecules is given by all DFT functionals, even though some are high-spin and other low-spin. The only exception is the Fe(III)(NH$_3$)$_6^{3+}$ complex, which has a high-spin ground-state experimentally and with OPBE, but for which other functionals were shown to fail by Deeth and Fey.[71] Not surprisingly, it was the standard pure DFT functionals, which tend to favor low-spin states, that failed. We will return to this issue (*vide infra*) when looking at which factors determine the actual spin ground-state of these iron complexes.

For these small and highly symmetric molecules, there are several spin-states that are formally Jahn−Teller active, which means that symmetry-lowering may result in more favorable energies for these spin-states. When using the QUILD program, this symmetry-lowering can consist of two parts, because one can separate the geometric symmetry from the electronic (orbitals) symmetry. For instance for Fe(II)-Cl$_4^{2-}$, the spin-states can be studied using (i) T_d symmetry for geometry and orbitals, (ii) T_d symmetry for geometry and C_{2v} symmetry for orbitals, or (iii) C_{2v} symmetry for both geometry and orbitals. Note that this symmetry-lowering is in particular beneficial for the intermediate (triplet) state,

2062 *J. Chem. Theory Comput., Vol. 4, No. 12, 2008*

Swart

Scheme 2. Challenging Iron Complexes Fe(phen)$_2$(NCS)$_2$, Fe(amp)$_2$Cl$_2$ (amp = 2-pyridylmethylamine), Fe(dpa)$_2^{2+}$ (dpa = di(2-pyridylmethyl)amine), and Fe([9]aneN$_3$)$_2$[a]

Fe(phen)$_2$(NCS)$_2$ **Fe(amp)$_2$Cl$_2$**

Fe([9]aneN$_3$)$_2$ **Fe(dpa)$_2^{2+}$**

[a] Hydrogens were omitted for clarity.

Table 4. Spin-State Splittings (kcal mol^{-1})[a] for Challenging Iron Complexes

compd	low spin	interm spin	high spin
Fe(phen)$_2$(NCS)$_2$	0	15.2 (19.3)	2.1 (6.7)
Fe(amp)$_2$Cl$_2$[b]	8.5 (10.7)	13.3 (7.9)	0
Fe(dpa)$_2^{2+c}$	0	11.8 (15.0)	2.3 (6.5)
Fe([9]aneN$_3$)$_2^{3+}$	0	13.8 (17.0)	2.9 (9.4)

[a] Relative to experimental spin ground-state, in parentheses the values when the solvent (methanol) is included. [b] amp = 2-pyridylmethylamine. [c] dpa = di(2-pyridylmethyl)amine.
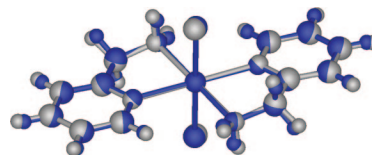

Figure 2. Overlay of experimental X-ray (in blue) and OPBE optimized (in gray) structure of Fe(amp)$_2$Cl$_2$.

Apart from the B3LYP and B3LYP* functionals, which were shown by Reiher[18] to fail for this complex, we were also interested in the performance of other recent functionals such as X3LYP[77] and M06.[78] Therefore, single-point energy calculations were performed where the energies of a large number of DFT functionals are calculated simultaneously (see Table S3 in the Supporting Information). These calculations showed that all hybrid functionals, except TPSSh[79,80] (with a ΔE_{HL} of +5.6 kcal mol^{-1}, i.e. ca. 10 kT), failed to provide the low-spin ground-state. Most standard (pure) functionals do provide the correct spin ground-state, but because they overstabilize low-spin states, they predict a too large energy separation between the low- and high-spin. In other words, they fail to describe the molecule as a spin-crossover compound. It should also be noted that the failure to predict the correct spin ground-state is not limited to hybrid functionals only. Also pure functionals like OLYP, HCTH, VS98, Becke00, OLAP3, and M06-L wrongly predict a high-spin ground-state (see Table S3).

Spin-State Splittings of Challenging Iron Complexes: Pyridylmethylamines. Westerhausen and co-workers[81] reported a series of iron complexes based on pyridylmethylamine ligands, which readily form complexes with iron halides in methanol. Here, we focus on two of the complexes reported in that study, Fe(amp)$_2$Cl$_2$ (amp = 2-pyridylmethylamine) and Fe(dpa)$_2^{2+}$ (dpa = di(2-pyridylmethyl)amine) (see Scheme 2). It was shown that Fe(amp)$_2$Cl$_2$ has a high-spin ground-state while Fe(dpa)$_2^{2+}$ has a low-spin ground-state. Both complexes are structurally highly similar, i.e. they have approximately an octahedral arrangement of the ligands around iron, and the only change in going from the monopma to the dipma complex is the replacement of two chloride ligands by pyridines.

We have optimized the geometries of the three spin-states for both these complexes, which result in the experimentally observed spin ground-state, i.e. a singlet for the dpa-complex and a quintet for the amp-complex (see Table 4). Also the obtained structures are in good agreement with the crystal structures (see Figure 2 for an overlay of the experimental and computed structures). For the amp-complex in the gas-phase, the Fe–Cl distances are a bit shorter (2.37 Å) and

which is spin-contaminated within T_d symmetry and a pure spin-state within C_{2v} symmetry. However, the energy that is gained by symmetry-lowering is only ca. 3 kcal·mol^{-1} (see Table 3).

Spin-State Splittings of Challenging Iron Complexes: Fe(phen)$_2$(NCS)$_2$. Reiher and co-workers[16] reparameterized the B3LYP functional to include only 15% of HF exchange (dubbed B3LYP*), based on the spin-state splittings for a number of Fe(II) complexes. Although this reduction of the amount of HF exchange does not seem to affect the performance for organic molecules,[17] and seems to be an improvement over B3LYP,[17] it still fails for some molecules.[18,19] Previously, it was already shown that B3LYP completely fails for spin-crossover compounds,[76] i.e. it usually predicts a high-spin ground-state, although at low temperatures a low-spin is observed experimentally. One typical example for which B3LYP (and B3LYP*) was shown to fail is the spin-crossover compound Fe(phen)$_2$(NCS)$_2$ (see Scheme 2).[18] The experimental value for the energy splitting between the low and high-spin state (ΔE_{HL}) is estimated to be of the order of 3 kT (ca. +1.8 kcal mol^{-1}) at 0 K, in order for the thermal spin transition to be viable. B3LYP and B3LYP* wrongly predict a high-spin state, with a ΔE_{HL} splitting of −8.0 kcal mol^{-1} (B3LYP) and −1.5 kcal mol^{-1} (B3LYP*).[18] The OPBE calculations, on the other hand, correctly show a low-spin ground-state for this complex, with the high-spin state higher in energy by 2.1 kcal mol^{-1}. This OPBE ΔE_{HL} splitting of 3.5 kT is therefore in perfect agreement with the estimated experimental value (*vide supra*).

Accurate Spin-State Energies

J. Chem. Theory Comput., Vol. 4, No. 12, 2008 **2063**

the Fe−N distances a bit longer (2.27−2.31) than observed in the crystal structure, where they are found at 2.50 and 2.19 Å respectively. However, by including the methanol solvent in the calculations (through a dielectric continuum model, COSMO) the iron-ligand distances match the ones from the crystal structure perfectly with values of 2.53 Å (Fe−Cl), 2.20 Å (Fe−N_{pyr}), and 2.23 Å (Fe−N_{am}). I.e., the molecule is severely Jahn−Teller distorted but in a similar fashion within the experiments and as optimized by OPBE. In the optimizations, the magnitude and orientation of the Jahn−Teller distortions came out the same, irrespective of the starting structure and initial distortions applied to it (see also Figure 2). The Fe−N distances in the dpa-complex are computed to be almost independent of the presence of the solvent, with values of 1.99 Å (Fe−N_{pyr}) and 2.01 Å (Fe−N_{am}) in the gas-phase and 1.98 Å (Fe−N_{pyr}) and 2.00 Å (Fe−N_{am}) in methanol. These distances are in excellent agreement with the crystal structure that puts them at 1.99 Å (Fe−N_{pyr}) and 2.03 Å (Fe−N_{am}). The origin of the change from high- to low-spin when going from the amp-complex to the dpa-complex is discussed below.

For these two complexes we also investigated the performance of a number of DFT functionals, with different results for each one (see Table S3 in the Supporting Information). For the high-spin complex Fe(amp)$_2$Cl$_2$, the standard DFT functionals like LDA, BP86, BLYP, or PBE fail and predict a low-spin ground-state instead. On the other hand, for the low-spin complex Fe(dpa)$_2$$^{2+}$, the hybrid functionals and some other ones (HCTH, OLAP3) wrongly predict a high-spin ground-state. In fact, apart from OPBE, OPerdew, and TPSSh, no other functional is able to correctly predict the spin ground-state of these challenging iron complexes. Most notably is the failure of XLYP, X3LYP (which were claimed to be the best functionals available for studying spin-state splittings[77]), and the M06 functionals, which predict the wrong spin ground-state for these complexes.

Spin-State Splittings of Challenging Iron Complexes: Cyclononanes. Wieghardt and co-workers[82] reported some time ago the first examples of low-spin iron complexes with all six donors as saturated nitrogens, which was based on the 1,4,7-triazacyclononane ligand [9]aneN$_3$. Here, we investigate the Fe(III) complex with two [9]aneN$_3$ ligands (see Scheme 2). As expected, OPBE correctly predicts a low-spin ground-state for this complex with the intermediate and high spin-state higher in energy by 14 and 3 kcal mol⁻¹ in the gas-phase, which increase to 17 and 10 kcal mol⁻¹ with the solvent present. The optimized structure with Fe−N distances of 2.03 Å in the gas phase and with 2.00 Å in methanol is also in perfect agreement with the crystal structure, that shows Fe−N distances of 1.98−2.01 Å. Therefore, like all other complexes, we see a consistent trend for the study on these challenging iron complexes, where the OPBE functional gives reliable and accurate results.

Rationalization of the Factors That Determine the Spin Ground-State of Iron Complexes. Now that the reliability of the OPBE functional for providing the spin ground-state of transition-metal complexes is established, the question remains to determine the factors that govern the spin ground-state of these transition-metal complexes. For

Table 5. Energy Decomposition Analysis (kcal mol⁻¹) for Small Complexes[a]

	Fe(II)Cl$_4$$^{2-}$[b]			Fe(II)CN$_6$$^{4-}$[c]		
	singlet	triplet[d]	quintet	singlet	triplet	quintet
ΔE_{prep}	618.4	567.7	493.0	1346.1	1217.9	1047.0
ΔE_{deform}	-	-	-	0.3	0.1	0.0
$\Delta E_{lig\text{-}lig}$	504.8	494.7	490.9	1232.3	1145.1	1044.9
ΔE_{valexc}	113.6	73.0	2.1	113.5	72.7	2.1
ΔE_{int}	−1134.5	−1109.6	−1090.1	−1722.2	−1541.6	−1383.6
ΔE_{Pauli}	160.6	138.7	127.1	320.5	173.9	73.2
ΔE_{elstat}	−1045.8	−1027.0	−1019.7	−1367.5	−1287.2	−1197.7
ΔE_{orbint}	−249.3	−221.1	−197.6	−675.3	−428.2	−259.1
A1	−117.0	−109.2	−91.1	−470.6	−278.0	−151.5
A2	−14.1	−18.1	−13.1	−30.4	−18.0	−10.8
B1	−82.2	−47.1	−46.7	−87.1	−64.8	−48.4
B2	−36.0	−46.7	−46.7	−87.1	−67.4	−48.4
ΔE_{total}	−516.1	−541.9	−597.1	−376.1	−323.7	−336.6

[a] Using C_{2v} symmetry for orbitals. [b] Using T_d symmetry for geometry. [c] Using O_h symmetry for geometry. [d] Spin-projection applied (see the Supporting Information).

Table 6. Energy Decomposition Analysis (kcal mol⁻¹) for Challenging Complexes[a]

	Fe(amp)$_2$Cl$_2$[b]			Fe(dpa)$_2$$^{2+}$[c]		
	singlet	triplet	quintet	singlet	triplet	quintet
ΔE_{prep}	265.9	209.0	125.6	196.5	134.6	48.7
ΔE_{deform}	15.4	9.8	8.1	29.5	20.3	14.6
$\Delta E_{lig\text{-}lig}$	136.9	126.5	115.4	53.4	41.6	32.0
ΔE_{valexc}	113.6	72.7	2.1	113.6	72.7	2.1
ΔE_{int}	−868.0	−806.5	−736.5	−558.4	−484.6	−408.3
ΔE_{Pauli}	251.7	205.2	136.3	266.5	250.8	133.7
ΔE_{elstat}	−651.5	−623.7	−596.7	−336.1	−309.1	−258.6
ΔE_{orbint}	−468.3	−387.9	−276.2	−488.9	−426.4	−283.4
Ag	−333.3	−262.5	−168.1	−345.5	−296.7	−169.5
Au	−135.0	−125.5	−108.1	−143.4	−129.7	−113.9
ΔE_{total}	−602.1	−597.5	−610.9	−361.9	−350.0	−359.6

[a] Using C_i symmetry for orbitals. [b] amp = 2-pyridylmethylamine. [c] dpa = di(2-pyridylmethyl)amine.

instance, why does the spin ground-state of the pyridylmethylamine complexes change from high-spin to low-spin if a chloride-ligand is changed by pyrimidine? And why do standard functionals have problems with predicting the high-spin ground-state of the complicated systems yet not with those for the small complexes?

In order to gain further insight, the bonding mechanism of a number of typical iron complexes from this study was analyzed in terms of an energy decomposition analysis of the Kohn−Sham molecular orbitals. The energy decomposition is reported in Table 5 for two small complexes, with a high-spin (Fe(II)Cl$_4$$^{2-}$) and a low-spin (Fe(II)CN$_6$$^{4-}$) ground-state, and in Table 6 for the pyridylmethylamine complexes. For the two small complexes, there is a striking difference in the preparation energy that is more than twice as large for Fe(II)CN$_6$$^{4-}$ than for Fe(II)Cl$_4$$^{2-}$. However, this energy difference results only from the ligand-ligand interactions ($\Delta E_{lig\text{-}lig}$), i.e. the electrostatic repulsion between the negatively charged ligands. Because the cyanide complex has six of them, their mutual repulsion is much larger. More importantly, this repulsive interaction is largest for the low-spin state, by 14 kcal·mol⁻¹ compared to the quintet state for the chloride complex and by ca. 187 kcal·mol⁻¹ for the cyanide complex. It results from the shorter metal−ligand

bond distances in the low spin-states, in which antibonding d-orbitals on iron are not occupied, in contrast to the higher spin-states where they are partially occupied.

The larger preparation energy for low spin-states is reinforced by Hund's rule of maximum multiplicity, which shows up in the valence excitation energy (ΔE_{valexc} in Tables 56). Hund's rule says that for atoms the state with the highest multiplet is lowest in energy, i.e. for the isolated iron(II) cation the quintet state is most favorable. Therefore, in order to make the low-spin iron complex, the iron(II) cation has to be changed from its favorable quintet state to the unfavorable singlet state. This change in multiplet state of the isolated cation (but with the occupation of the orbitals it attains in the molecule, see the Computational Details section) costs around 114 kcal·mol^{-1} (see Table 5). Taken together with the (repulsive) ligand-ligand interactions, the low spin-state has a much larger preparation energy than higher spin-states, of ca. 125 kcal·mol^{-1} for the chloride complex and ca. 300 kcal·mol^{-1} for the cyanide complex.

The interaction between the iron cation and its ligands on the other hand favors the low spin-states considerably. For Fe(II)Cl$_4^{2-}$, the interaction energy (ΔE_{int}) is 44 kcal·mol^{-1} larger for the singlet than for the quintet state (see Table 5), which results almost entirely (52 kcal·mol^{-1}) from covalent interactions (ΔE_{orbint}). The sum of the Pauli repulsion (ΔE_{Pauli}) and electrostatic interactions (ΔE_{elstat}) contributes only ca. 8 kcal·mol^{-1} to this energy difference. However, the difference in interaction energy of ca. 44 kcal·mol^{-1} in favor of the low spin-state is not sufficient to overcome the difference in preparation energy (125 kcal·mol^{-1}), and as a result this chloride complex has a high-spin ground-state. For the Fe(II)CN$_6^{4-}$ complex, the interaction energy (ΔE_{int}) is significantly larger than that for the chloride complex (ca. 588 kcal·mol^{-1} for the singlet state, see Table 5) and is ca. 338 kcal·mol^{-1} larger for the low spin-state compared to the high spin-state. Again, this difference results mainly from the covalent interactions (ΔE_{orbint}) which are 416 kcal·mol^{-1} more favorable for the singlet state, with a much smaller contribution (78 kcal·mol^{-1}) from the steric interactions (sum of ΔE_{Pauli} and ΔE_{elstat}). Therefore, for the cyanide complex the favorable difference in interaction energy is sufficiently large to overcome the unfavorable difference in preparation energy between the singlet and quintet, and hence a low-spin ground-state is observed with the quintet higher in energy by ca. 40 kcal/mol.

The interplay between the interaction energy and the preparation energy is for these small complexes severely unbalanced, which results in a clearly defined spin ground-state for either of these two small complexes. Consequently, the other DFT functionals do provide the correct ground-state preferences. This however changes for the challenging complexes where the interplay between interaction energy versus preparation energy is more subtle.

For the pyridylmethylamine complexes Fe(amp)$_2$Cl$_2$ and Fe(dpa)$^{2+}$, both the absolute values of the interaction energies as well as the differences of them for the three spin states is much smaller than for the small complexes (see Table 6). Similar to these latter complexes, also for the pyridylmethylamine complexes is the preparation energy the largest for the low-spin singlet state. For all three components of the preparation energy (ΔE_{deform}, $\Delta E_{lig-lig}$, ΔE_{valexc}) is the largest value observed for the low spin-state. This larger preparation energy for the low spin-state is counteracted by a larger interaction energy, in a similar fashion to the small complexes (*vide supra*). The difference in interaction energy ($\Delta\Delta E_{int}$) results again mainly from the covalent interactions ($\Delta\Delta E_{orbint}$, 192 and 206 kcal·mol^{-1}, see Table 6), with a smaller contribution from the steric interactions (sum of $\Delta\Delta E_{Pauli}$ and $\Delta\Delta E_{elstat}$) of ca. 55−60 kcal·mol^{-1}. The more favorable orbital interactions occur mainly in those irreps (A$_1$ for the small complexes, A$_g$ here) that contain the iron d-orbitals, which are unoccupied in the low-spin and partially occupied in high-spin states.

The balance between the preparation of the fragments, and the subsequent interaction between these, then determines the actual spin state observed. Thus, for Fe(amp)$_2$Cl$_2$ the interaction energy difference ($\Delta\Delta E_{int}$, see Table 6) between singlet and quintet (131 kcal·mol^{-1}) is too small to overcome the difference in preparation energy ($\Delta\Delta E_{prep}$, 140 kcal·mol^{-1}), and hence this molecule has a high-spin ground-state. On the other hand, for Fe(dpa)$^{2+}$ the interaction energy difference (150 kcal·mol^{-1}) is sufficiently large to overcome the unfavorable preparation energy ($\Delta\Delta E_{prep}$, 148 kcal·mol^{-1}), and the molecule has a low-spin ground-state. Therefore, the spin ground-state of these iron complexes is determined completely by a delicate compromise[19] between Hund's rule of maximum multiplicity, which favors high spin-states, and metal−ligand bonding that favors low spin-states.

Conclusions

The performance of the OPBE functional has been checked for the geometries and relaxed (adiabatic) spin-state energies of transition-metal complexes. The performance for the geometry was checked for the bond-lengths of transition-metal (di)halides, which was shown[68] to be representative for a much larger and more diverse set of 32 metal complexes. The accuracy of the OPBE bond lengths is close to that of the best-performing DFT functionals and significantly better than most others such as B3LYP.

The performance of OPBE for the relaxed spin-state energies has been checked for a set of small complexes, a set of benchmark systems where highly accurate CASPT2 energies are available as reference, and a set of challenging complexes such as the spin-crossover compound Fe(phen)$_2$-(NCS)$_2$ and pyridylmethylamine complexes. The failure of hybrid functionals such as B3LYP and B3LYP* for these low-spin complexes has been reported before[18] and is confirmed here, including for other (newer) functionals such as X3LYP and M06. In contrast, the OPBE functional gives excellent results in all cases. For the set of benchmark systems, the difference between the reference CASPT2 data and the OPBE energies (1−2 kcal·mol^{-1}) is an order of magnitude smaller than those of other functionals (9−15 kcal·mol^{-1}), and it lies well within the estimated accuracy (3 kcal·mol^{-1}) of the reference CASPT2 data.

In order to gain insight in the factors that determine the spin ground-state of transition-metal complexes, the chemical bonding for a number of iron complexes is analyzed in terms

of an energy decomposition analysis. From this analysis, it becomes clear that two opposing forces act on the metal, one that prefers a high spin-state (Hund's rule of maximum multiplicity) which is counteracted by the metal–ligand bonding that prefers low spin-states. The interplay between these two opposing effects then determines the spin ground-state of the metal-complex.

Supporting Information Available: Details of the spin-projection for the triplet state of $Fe(II)Cl_4^{2-}$, interaction and preparation energies corrected for self-consistency of the metal cation (see computational details), additional energy decomposition analyses, and Cartesian coordinates of the challenging complexes. This material is available free of charge via the Internet at http://pubs.acs.org.

References

(1) Swart, M.; Groenhof, A. R.; Ehlers, A. W.; Lammertsma, K. *J. Phys. Chem. A* **2004**, *108*, 5479.

(2) Sellmann, D.; Soglowek, W.; Knoch, F.; Ritter, G.; Dengler, J. *Inorg. Chem.* **1992**, *31*, 3711.

(3) Limberg, C. *Angew. Chem., Int. Ed.* **2003**, *42*, 5932.

(4) Denisov, I. G.; Makris, T. M.; Sligar, S. G.; Schlichting, I. *Chem. Rev.* **2005**, *105*, 2253.

(5) Shaik, S.; Kumar, D.; de Visser, S. P.; Altun, A.; Thiel, W. *Chem. Rev.* **2005**, *105*, 2279.

(6) Groenhof, A. R.; Ehlers, A. W.; Lammertsma, K. *J. Am. Chem. Soc.* **2007**, *129*, 6204.

(7) *Spin Crossover in Transition Metal Complexes I-III*; Gütlich, P., Goodwin, H. A., Eds.;Springer: Berlin/Heidelberg, Germany, 2004; Vols. 233–235 of Topics in Current Chemistry series.

(8) Koch, W.; Holthausen, M. C. *A Chemist's Guide to Density Functional Theory*; Wiley-VCH: Weinheim, Germany, 2000.

(9) Vosko, S. H.; Wilk, L.; Nusair, M. *Can. J. Phys* **1980**, *58*, 1200.

(10) Becke, A. D. *Phys. Rev. A* **1988**, *38*, 3098.

(11) Lee, C.; Yang, W.; Parr, R. G. *Phys. Rev. B* **1988**, *37*, 785.

(12) Perdew, J. P.; Burke, K.; Ernzerhof, M. *Phys. Rev. Lett.* **1996**, *77*, 3865.

(13) Stephens, P. J.; Devlin, F. J.; Chabalowski, C. F.; Frisch, M. J. *J. Phys. Chem.* **1994**, *45*, 11623.

(14) Becke, A. D. *J. Chem. Phys.* **1993**, *98*, 5648.

(15) Perdew, J. P.; Emzerhof, M.; Burke, K. *J. Chem. Phys.* **1996**, *105*, 9982.

(16) Reiher, M.; Salomon, O.; Hess, B. A. *Theor. Chem. Acc.* **2001**, *107*, 48.

(17) Salomon, O.; Reiher, M.; Hess, B. A. *J. Chem. Phys.* **2002**, *117*, 4729.

(18) Reiher, M. *Inorg. Chem.* **2002**, *41*, 6928.

(19) Swart, M. *Inorg. Chim. Acta* **2007**, *360*, 179.

(20) Güell, M.; Luis, J. M.; Solà, M.; Swart, M. *J. Phys. Chem. A* **2008**, *112*, 6384.

(21) Harvey, J. N. *Struct. Bonding (Berlin)* **2004**, *112*, 151.

(22) Conradie, J.; Ghosh, A. *J. Chem. Theory Comput.* **2007**, *3*, 689.

(23) Conradie, J.; Ghosh, A. *J. Phys. Chem. B* **2007**, *111*, 12621.

(24) Handy, N. C.; Cohen, A. J. *Mol. Phys.* **2001**, *99*, 403.

(25) Swart, M.; Ehlers, A. W.; Lammertsma, K. *Mol. Phys.* **2004**, *102*, 2467.

(26) Zhang, Y.-Q.; Luo, C.-L. *J. Phys. Chem. A* **2006**, *110*, 5096.

(27) Zhang, Y.; Wu, A.; Xu, X.; Yan, Y. *Chem. Phys. Lett.* **2006**, *421*, 383.

(28) Wu, A.; Zhang, Y.; Xu, X.; Yan, Y. *J. Comput. Chem.* **2007**, *28*, 2431.

(29) Wasbotten, I.; Ghosh, A. *Inorg. Chem.* **2006**, *45*, 4910.

(30) Derat, E.; Kumar, D.; Neumann, R.; Shaik, S. *Inorg. Chem.* **2006**, *45*, 8655.

(31) Romo, S.; Fernández, J. A.; Maestre, J. M.; Keita, B.; Nadjo, L.; de Graaf, C.; Poblet, J. M. *Inorg. Chem.* **2007**, *46*, 4022.

(32) Rong, C.; Lian, S.; Yin, D.; Shen, B.; Zhong, A.; Bartolotti, L.; Liu, S. *J. Chem. Phys.* **2006**, *125*, 174102.

(33) Liao, M.-S.; Watts, J. D.; Huang, M.-J. *J. Comput. Chem.* **2006**, *27*, 1577.

(34) Liao, M.-S.; Watts, J. D.; Huang, M.-J. *J. Phys. Chem. A* **2007**, *111*, 5927.

(35) Zein, S.; Borshch, S. A.; Fleurat-Lessard, P.; Casida, M. E.; Chermette, H. *J. Chem. Phys.* **2007**, *126*, 014105.

(36) Swart, M.; Solà, M.; Bickelhaupt, F. M. *J. Comput. Chem.* **2007**, *28*, 1551.

(37) Han, W. G.; Noodleman, L. *Inorg. Chim. Acta* **2008**, *361*, 973.

(38) Han, W. G.; Noodleman, L. *Inorg. Chem.* **2008**, *47*, 2975.

(39) Ghosh, A. *J. Biol. Inorg. Chem.* **2006**, *11*, 671.

(40) Ghosh, A. *J. Biol. Inorg. Chem.* **2006**, *11*, 712.

(41) Tangen, E.; Conradie, J.; Ghosh, A. *J. Chem. Theory Comput.* **2007**, *3*, 448.

(42) Conradie, J.; Quarless, D. A.; Hsu, H. F.; Harrop, T. C.; Lippard, S. J.; Koch, S. A.; Ghosh, A. *J. Am. Chem. Soc.* **2007**, *129*, 10446.

(43) Wasbotten, I. H.; Ghosh, A. *Inorg. Chem.* **2007**, *46*, 7890.

(44) Conradie, J.; Ghosh, A. *J. Chem. Theory Comput.* **2007**, *3*, 689.

(45) Conradie, J.; Wondimagegn, T.; Ghosh, A. *J. Phys. Chem. B* **2008**, *112*, 1053.

(46) te Velde, G.; Bickelhaupt, F. M.; Baerends, E. J.; Fonseca Guerra, C.; van Gisbergen, S. J. A.; Snijders, J. G.; Ziegler, T. *J. Comput. Chem.* **2001**, *22*, 931.

(47) Baerends, E. J.; Autschbach, J.; Bérces, A.; Berger, J. A.; Bickelhaupt, F. M.; Bo, C.; de Boeij, P. L.; Boerrigter, P. M.; Cavallo, L.; Chong, D. P.; Deng, L.; Dickson, R. M.; Ellis, D. E.; van Faassen, M.; Fan, L.; Fischer, T. H.; Fonseca Guerra, C.; van Gisbergen, S. J. A.; Groeneveld, J. A.; Gritsenko, O. V.; Grüning, M.; Harris, F. E.; van den Hoek, P.; Jacob, C. R.; Jacobsen, H.; Jensen, L.; Kadantsev, E. S.; van Kessel, G.; Klooster, R.; Kootstra, F.; van Lenthe, E.; McCormack, D. A.; Michalak, A.; Neugebauer, J.; Nicu, V. P.;

Osinga, V. P.; Patchkovskii, S.; Philipsen, P. H. T.; Post, D.; Pye, C. C.; Ravenek, W.; Romaniello, P.; Ros, P.; Schipper, P. R. T.; Schreckenbach, G.; Snijders, J. G.; Solà, M.; Swart, M.; Swerhone, D.; te Velde, G.; Vernooijs, P.; Versluis, L.; Visscher, L.; Visser, O.; Wang, F.; Wesolowski, T. A.; van Wezenbeek, E. M.; Wiesenekker, G.; Wolff, S. K.; Woo, T. K.; Yakovlev, A. L.; Ziegler, T. *ADF 2007.01*; SCM: Amsterdam, The Netherlands, 2007.

(48) van Lenthe, E.; Baerends, E. J. *J. Comput. Chem.* **2003**, *24*, 1142.

(49) Swart, M.; Snijders, J. G. *Theor. Chem. Acc.* **2003**, *110*, 34.

(50) Perdew, J. P.; Burke, K.; Ernzerhof, M. *Phys. Rev. Lett.* **1996**, *77*, 3865.

(51) Perdew, J. P.; Burke, K.; Wang, Y. *Phys. Rev. B* **1996**, *54*, 16533.

(52) Swart, M.; Bickelhaupt, F. M. *Int. J. Quantum Chem.* **2006**, *106*, 2536.

(53) Swart, M.; Bickelhaupt, F. M. *J. Comput. Chem.* **2008**, *29*, 724.

(54) Bylaska, E. J.; de Jong, W. A.; Kowalski, K.; Straatsma, T. P.; Valiev, M.; Wang, D.; Apra, E.; Windus, T. L.; Hirata, S.; Hackler, M. T.; Zhao, Y.; Fan, P.-D.; Harrison, R. J.; Dupuis, M.; Smith, D. M. A.; Nieplocha, J.; Tipparaju, V.; Krishnan, M.; Auer, A. A.; Nooijen, M.; Brown, E.; Cisneros, G.; Fann, G. I.; Fruchtl, H.; Garza, J.; Hirao, K.; Kendall, R.; Nichols, J. A.; Tsemekhman, K.; Wolinski, K.; Anchell, J.; Bernholdt, D.; Borowski, P.; Clark, T.; Clerc, D.; Dachsel, H.; Deegan, M.; Dyall, K.; Elwood, D.; Glendening, E.; Gutowski, M.; Hess, A.; Jaffe, J.; Johnson, B.; Ju, J.; Kobayashi, R.; Kutteh, R.; Lin, Z.; Littlefield, R.; Long, X.; Meng, B.; Nakajima, T.; Niu, S.; Pollack, L.; Rosing, M.; Sandrone, G.; Stave, M.; Taylor, H.; Thomas, G.; van Lenthe, J.; Wong, A.; Zhang. Z. *NWChem, A Computational Chemistry Package for Parallel Computers*; Pacific Northwest National Laboratory: Richland, WA, 2006.

(55) Environmental and Molecular Sciences Laboratory. Basis set order form. http://www.emsl.pnl.gov/forms/basisform.html (accessed Feb 8, 2008).

(56) Klamt, A.; Schüürmann, G. *J. Chem. Soc., Perkin Trans. 2* **1993**, 799.

(57) Pye, C. C.; Ziegler, T. *Theor. Chem. Acc.* **1999**, *101*, 396.

(58) Bon, R. S.; van Vliet, B.; Sprenkels, N. E.; Schmitz, R. F.; de Kanter, F. J. J.; Stevens, C. V.; Swart, M.; Bickelhaupt, F. M.; Groen, M. B.; Orru, R. V. A. *J. Org. Chem.* **2005**, *70*, 3542.

(59) Swart, M.; Rösler, E.; Bickelhaupt, F. M. *Eur. J. Inorg. Chem.* **2007**, 3646.

(60) Bickelhaupt, F. M.; Baerends, E. J. In *Reviews in Computational Chemistry, Vol. 15*; Wiley-VCH: New York, 2000; Vol. 15, p 1.

(61) Baerends, E. J.; Branchadell, V.; Sodupe, M. *Chem. Phys. Lett.* **1997**, *265*, 481.

(62) Fouqueau, A.; Mer, S.; Casida, M. E.; Daku, L. M. L.; Hauser, A.; Mineva, T.; Neese, F. *J. Chem. Phys.* **2004**, *120*, 9473.

(63) Morokuma, K. *Acc. Chem. Res.* **1977**, *10*, 294.

(64) Ziegler, T.; Rauk, A. *Inorg. Chem.* **1979**, *18*, 1558.

(65) Ziegler, T.; Rauk, A. *Inorg. Chem.* **1979**, *18*, 1755.

(66) Groenhof, A. R.; Swart, M.; Ehlers, A. W.; Lammertsma, K. *J. Phys. Chem. A* **2005**, *109*, 3411.

(67) Wittbrodt, J. M.; Schlegel, H. B. *J. Chem. Phys.* **1996**, *105*, 6574.

(68) Bühl, M.; Kabrede, H. *J. Chem. Theory Comput.* **2006**, *2*, 1282.

(69) Pierloot, K.; Vancoillie, S. *J. Chem. Phys.* **2006**, *125*, 124303.

(70) Pierloot, K.; Vancoillie, S. *J. Chem. Phys.* **2008**, *128*, 034104.

(71) Deeth, R. J.; Fey, N. *J. Comput. Chem.* **2004**, *25*, 1840.

(72) Fouqueau, A.; Casida, M. E.; Daku, L. M. L.; Hauser, A.; Neese, F. *J. Chem. Phys.* **2005**, 122.

(73) Lawson Daku, L. M.; Vargas, A.; Hauser, A.; Fouqueau, A.; Casida, M. E. *ChemPhysChem* **2005**, *6*, 1393.

(74) Neese, F. *Inorg. Chim. Acta* **2002**, *337*, 181.

(75) Filatov, M. *J. Chem. Phys.* **2007**, *127*, 084101.

(76) Paulsen, H.; Duelund, L.; Winkler, H.; Toftlund, H.; Trautwein, A. X. *Inorg. Chem.* **2001**, *40*, 2201.

(77) Xu, X.; Goddard III, W. A. *Proc. Natl. Acad. Sci. U.S.A.* **2004**, *101*, 2673.

(78) Zhao, Y.; Truhlar, D. G. *Theor. Chem. Acc.* **2008**, *120*, 215.

(79) Tao, J. M.; Perdew, J. P.; Staroverov, V. N.; Scuseria, G. E. *Phys. Rev. Lett.* **2003**, *91*, 146401.

(80) Staroverov, V. N.; Scuseria, G. E.; Tao, J.; Perdew, J. P. *J. Chem. Phys.* **2003**, *119*, 12129.

(81) Malassa, A.; Görls, H.; Buchholz, A.; Plass, W.; Westerhausen, M. *Z. Anorg. Allg. Chem.* **2006**, *632*, 2355.

(82) Boeyens, J. C. A.; Forbes, A. G. S.; Hancock, R. D.; Wieghardt, K. *Inorg. Chem.* **1985**, *24*, 2926.

CT800277A